Invited paper presented at the
Davis International Conference
on Inclusive Reactions, University of
California, Davis, California
February 4 and 5, 1972

LBL-747

A HYBRID SPARK CHAMBER-BUBBLE CHAMBER EXPERIMENT TO STUDY $\pi^- p$ INTERACTIONS AT 14 GeV/c; A PROGRESS REPORT*

A. Dzierba, A. Firestone, W. T. Ford, R. Gomez, P. Oddone,
C. W. Peck, J. Power, C. Rosenfeld

California Institute of Technology
Pasadena, California 91109

and

R. Ely, D. F. Grether

E. O. Lawrence Berkeley Laboratory
University of California
Berkeley, California 94720

Presented by: D. F. Grether

*Work performed under the auspices of the U. S. Atomic Energy Commission.

We report on an experiment that is peripheral to the main thrust of the conference since it is not designed to study inclusive processes. The reason for discussing it here is that it is a hybrid spark chamber-bubble chamber experiment and is thus a prototype for a number of experiments proposed for the 30" chamber at NAL. The experiment is a joint Cal Tech-Berkeley effort to study diffractive dissociation of the nucleon with high statistics and good resolution in the reaction $\pi^- p \to \pi^- + X$. The data was taken at SLAC during the spring and summer of 1971. We defer the discussion of the physics of the experiment to a future time when we will have analyzed substantially more of the data than to date. For the present we restrict ourselves to briefly explaining the nature of the experiment and showing evidence that the experiment is a technical success.

The layout of the experiment is shown in Fig. 1a. A 14 GeV/c π^- beam is incident upon the SLAC 40" hydrogen bubble chamber. Undeflected beam particles and high momentum particles from interactions exit the chamber through a thin window and pass through an external spectrometer. The spectrometer has four stations of magnetostrictive wire plane spark chambers and a large aperture magnet. (The unscattered beam passes through dead spots in the chambers.) The spark chamber readout is fed to an online computer that reconstructs the tracks and calculates (approximately) the missing mass from an assumed interaction in the bubble chamber. The computer triggers the bubble chamber lights (takes a picture) if $1.1 \leq mm \leq 3.8$ GeV. This cut excludes most elastic scatters and includes inelastic events in the diffractive dissociation region. The geometry of the system limits the momentum transfer to

$.01 \leq t \leq .6$ GeV/c^2. The bubble chamber was expanded typically 4 times/second and on the average a picture was taken every 17 expansions. Altogether some 400,000 pictures were taken which corresponds to some 7 million expansions of the chamber. Allowing for triggers by interactions outside the fiducial volume or in the windows of the bubble chamber, π decays, some residual elastic scatters, and the like we expect to obtain more than 100,000 events in the diffractive dissociation region.

The motivation for the external spectrometer was not only to trigger the bubble chamber but to improve the resolution by providing an accurate measure of the high momentum outgoing π^-. The spectrometer is capable of measuring a 14 GeV/c track to ± 1/2%, a good match to the beam momentum width of ± 1/4%. The error in the bubble chamber measurement is typically 10-30%. To accomplish this improvement in resolution for a given event measured in the bubble chamber, we must match the high momentum secondary track in the event to the same track as measured by the spark chambers (and recorded on magnetic tape). Avoiding accidental matches is important since there are usually several tracks in the spark chambers and there are of course events in the bubble chamber for which there is no corresponding spark chamber track. The matching process is indicated in Fig. 1b. A spark chamber track is extrapolated from station 1 back through the fringe field of the bubble chamber magnet to the downstream end of the bubble chamber track. The tracks must then match in the azimuth angle, ϕ, the dip angle, λ, the position coordinate, x, which is perpendicular to the beam tracks and magnetic field, and the position coordinate, z, which is parallel to the magnetic field. Differences between the bubble chamber and spark chamber values are histogrammed in Fig. 2 for a sample of events. The dotted histograms are for the same bubble chamber events compared to spark chamber tracks from a wrong frame and thus show the shape of the distributions for accidental matches. These latter distributions are rather flat and show that the peaks in the "right frame" distributions originate from correct matches. The rms widths of the peaks are: for λ, ~ 3 mr; for ϕ, ~ 1.5 mr; for x, ~ 1 mm; and for z, ~ 2 mm. The comparisons of the four variables, together with estimates of the errors, are used to form a χ^2 with four degrees of freedom. The distributions for the right frame (solid histogram) and wrong frame (dotted histogram) comparisons are shown in Fig. 3a. The negligible number of events in the wrong frame distributions shows that the χ^2 provides an excellent discrimination against accidental matches.

Once matched, we combine the bubble chamber measurement of the event and the spark chamber measurement of the high momentum track into a "hybrid" measurement of the event. We illustrate the effect of the hybrid measurement by considering two-prong events from a sample of film for which the bubble chamber was triggered by elastic as well as inelastic scatters. Fig. 3b shows the distribution of missing mass recoiling off the outgoing π^-. The solid histogram is for the hybrid measurement and shows a proton peak from the elastic scatters. The dotted histogram is for the bubble chamber only measurement; the proton peak has been spread out to the point of disappearing. Somewhat more relevant to the physics of the experiment is the question of to what extent the increased resolution provided by the hybrid measurement allows separation of the single π^0 from multiple π^0 events, and neutron from neutron + π^0 events. We show in Fig. 3c a missing mass distribution for neutral particles for a sample of two prong events in which the positive track has been identified as a proton by ionization; Fig. 3d shows a similar distribution for the positive track identified as a π^+. The π^0 peak in Fig. 3c and neutron peak in 3d are clearly discernable. For reference, two π^0 threshold in 3c and neutron + π^0 threshold in 3d are indicated by small arrows. The same distributions using the bubble chamber measurements (not shown) do not have either the π^0 or neutron peak.

In conclusion, the experiment is a technical success. The external spectrometer triggered the bubble chamber with relatively high efficiency and provides much improved resolution over bubble chamber measurements alone. We are currently measuring and processing the bubble chamber events and anticipate physics results in the not-too-distant future.

FIGURE LEGENDS

Fig. 1. (a) Top view of experimental layout.

(b) Side view of bubble chamber and station 1 of spark chambers, illustrating the track matching process and coordinate system used.

Fig. 2. Comparisons of bubble chamber and spark chamber measurements of the downstream end of a sample of bubble chamber tracks. The dotted histograms are for the "wrong frame" comparisons.

Fig. 3. (a) χ^2 from comparisons in Fig. 2. The dotted histogram is for the "wrong frame" comparisons.

(b) Missing mass recoiling off the outgoing π^- for a sample of elastic and inelastic two-prongs. The solid histogram is for the hybrid measurements; the dotted for the bubble chamber measurements.

(c) Missing mass squared of neutral particles for two-prong events with the positive track identified as a proton by ionization. The arrow indicates two π^0 threshold.

(d) Same as (c) but for the positive track identified as a π^+. The arrow indicates neutron + π^0 threshold.

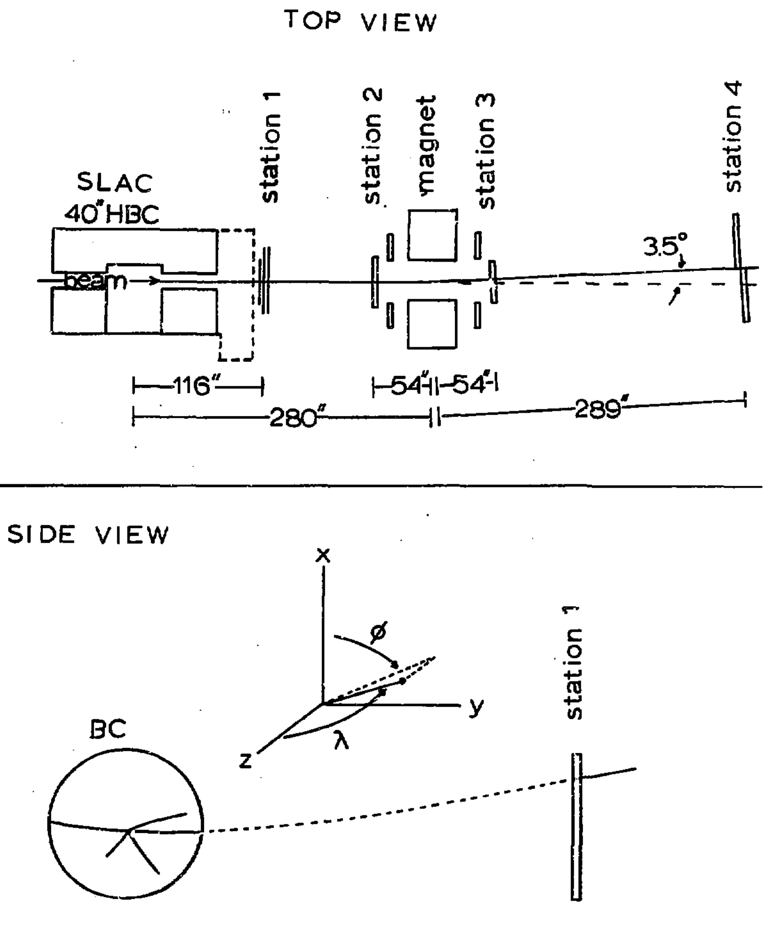

XBL 723-409

Fig. 1

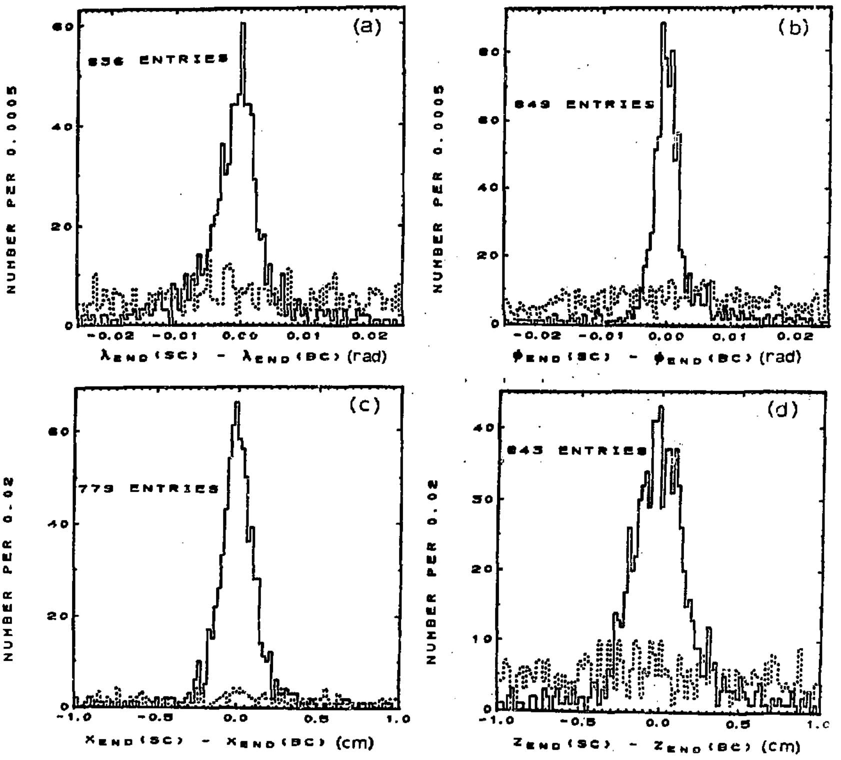

XBL 723-407

Fig. 2

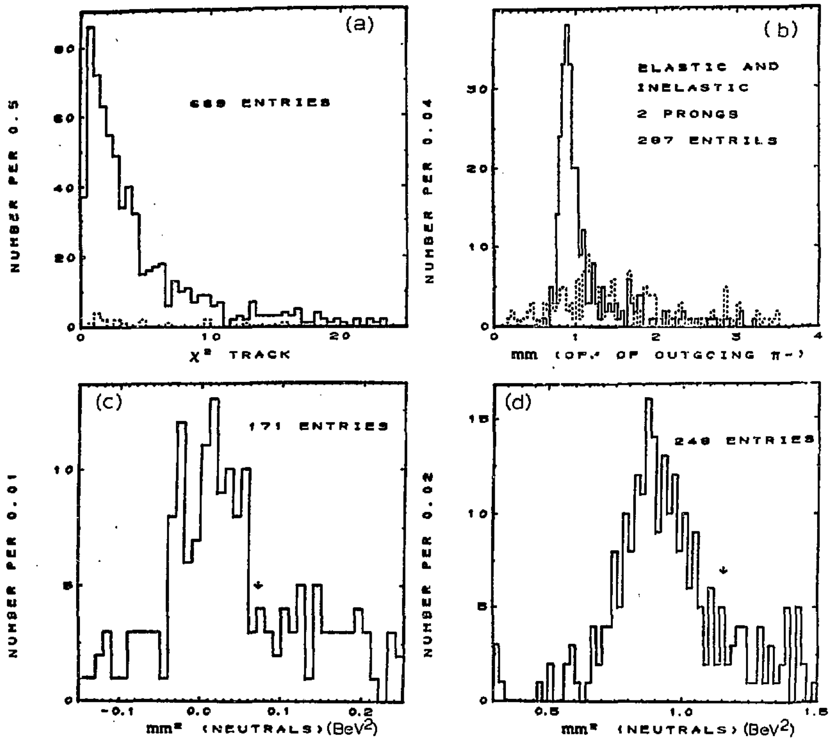

XBL 723-408

Fig. 3